

# A study of complex effects of alumina addition on conductivity of stabilised zirconia

Dorthe Lybye\*, Yi-Lin Liu

*Materials Research Department, Risø National Laboratory, DK-4000 Roskilde, Denmark*

Available online 22 August 2005

## Abstract

When zirconia is used as electrolyte material in intermediate temperature solid oxide fuel cells, the influence of impurities on conductivity becomes more significant than at high temperature. It is, therefore, important to understand the effect of impurities and if possible remove them. SiO<sub>2</sub> is an impurity known to be present in zirconia and to have a negative effect on conductivity. Since the early 1980s, several groups have reported Al<sub>2</sub>O<sub>3</sub> to act as a scavenger of SiO<sub>2</sub> in zirconia. However, conflicting results have been obtained. Both increases and decreases in grain boundary conductivity have been found along with a decrease in grain interior conductivity. The effect of Al<sub>2</sub>O<sub>3</sub> seems to be dependent on the ratio between Al<sub>2</sub>O<sub>3</sub> and SiO<sub>2</sub> in the material, and on the concentration and the distribution of Al<sub>2</sub>O<sub>3</sub> in zirconia. Here, the results described in literature are reviewed and compared with new results obtained on Sc<sub>0.16</sub>Y<sub>0.04</sub>Zr<sub>0.80</sub>O<sub>1.9</sub> and Tosoh TZ8Y. The samples were investigated with respect to conductivity (impedance spectroscopy) and microstructure (scanning and transmission electron microscopy) in order not only to find a trend but also to understand the mechanism of Al<sub>2</sub>O<sub>3</sub> addition.

© 2005 Elsevier Ltd. All rights reserved.

**Keywords:** Grain boundaries; Impurities; Ionic conductivity; ZrO<sub>2</sub>; Fuel cells

## 1. Introduction

Alumina is added to stabilised zirconia for several reasons; as a sintering aid,<sup>1</sup> as a scavenger of Si,<sup>2,3</sup> to improve strength<sup>4</sup> of stabilised zirconia and to lower the thermal expansion coefficient.<sup>5</sup> This has resulted in several papers on the effect of alumina addition. In the present paper, the focus will be on the effects of alumina as a scavenger, i.e. the effects on conductivity. The results reported in literature are reviewed. An explanation for the contradiction between these results is proposed and verified by new experimental results obtained on Sc<sub>0.16</sub>Y<sub>0.04</sub>Zr<sub>0.80</sub>O<sub>2-δ</sub> and Tosoh TZ8Y.

Since the early 1980s<sup>2</sup> it has been reported that adding alumina to stabilised zirconia has a positive effect on conductivity. However, conflicting results have been obtained on alumina doped yttria stabilised zirconia. Both increases<sup>2</sup> and decreases<sup>6,7</sup> in grain boundary conductivity have been

reported along with a decrease<sup>8</sup> and increase<sup>9</sup> in bulk conductivity due to alumina addition. A direct comparison of these literature data is very difficult since material and process parameters such as sintering temperature and time, powder supplier, powder preparation, amount of dopants and amount of Al<sub>2</sub>O<sub>3</sub> added differ from each other. The sintering temperature varies between 1350 °C<sup>10</sup> and 1700 °C.<sup>11</sup> The sintering time varies between 2 h<sup>12</sup> and 30 h.<sup>10</sup> Powder comes from different suppliers or is made in the laboratory resulting in different content of Si and other impurities. The amount and type of impurities in the powder are essential when the aim is to understand the formation and behaviour of the grain boundary glass phases found in yttria stabilised zirconia.

Adding alumina to zirconia influences both bulk and grain boundary conductivity. The former is depending on alumina solubility in zirconia and the latter is mainly depending on how alumina changes the grain boundary impurity phases. Firstly, alumina is only sparingly soluble in stabilised zirconia. The solubility is approx. 0.6 mol% Al when sintered at 1500 °C for 24 h.<sup>8</sup> At 1300 °C, the solubility of Al has decreased to 0.1 mol%.<sup>6</sup> The low solubility, however, seems

\* Corresponding author. Tel.: +45 4677 5847; fax: +45 4677 5758.

E-mail address: [dorthe.lybye@risoe.dk](mailto:dorthe.lybye@risoe.dk) (D. Lybye).

to be an advantage. When alumina is added to zirconia, the decrease in bulk conductivity can be ascribed to the solution of Al in the lattice. The ionic radius of aluminium ( $r_{\text{Al}^{3+}} = 0.535$  at CN=6)<sup>13</sup> is much smaller than the radius of the zirconium ions ( $r_{\text{Zr}^{4+}} = 0.84$  at CN=8).<sup>13</sup> This causes local stresses in the lattice, traps vacancies and reduces conductivity of the bulk. The ionic size mismatch is also the reason for the low solubility. Secondly, there is agreement in literature that Al acts as a scavenger for Si impurities having a positive effect on conductivity. Therefore, the net effect of alumina on the conductivity has to be understood as a combined effect. From this point of view the reported decreases in conductivity are likely to be caused by too high amounts of Al added compared to the amount necessary to scavenge a given amount of Si. In this case Al acts as an impurity like other undissolvable ions and accumulates in the grain boundaries.

In the present work, the effects of alumina added with respect to the amount of impurities (Si, Na, Ca, K, ...) in stabilised zirconia have been studied. In this study the materials ( $\text{Sc}_{0.16}\text{Y}_{0.04}\text{Zr}_{0.80}\text{O}_{2-\delta}$  and Tosoh TZ8Y) and the processing parameters are well controlled and therefore, the results are more relevant and comparable. The samples are investigated with respect to conductivity (impedance spectroscopy) and microstructure (scanning and transmission electron microscopy) in order not only to find a trend but also to understand the mechanism of  $\text{Al}_2\text{O}_3$  addition. In this work a low amount of alumina (0–2 at.% Al) is added when comparison to literature is made.

## 2. Experimental

Samples of  $\text{Sc}_{0.16}\text{Y}_{0.04}\text{Zr}_{0.80}\text{O}_{2-\delta}$ , Viking Chemicals, (ScYSZ) with 0, 0.5, 1 and 2 at.% Al have been prepared as well as samples of Tosoh TZ8Y with 0, 0.5 and 2 at.% Al. The impurity level of the zirconia raw materials has been measured by glow discharge mass spectrometry (GDMS) used for analysis of trace and ultra-trace element constituents of inorganic samples. By GDMS powder is atomised by sputtering in low-pressure DC plasma and the ionised atoms are extracted into a mass spectrometer for separation and detection.

Aluminium was added as boehmite,  $\text{AlO}(\text{OH})$ , Catapal B, and wet ball milled into the zirconia powder for 24 h. The powders without additions were ball milled accordingly in order not to differ in nominal grain size or amount of impurities introduced by ball milling. The powders were then dried and pressed isostatically into pellets. Pellets for conductivity measurements were sintered at 1500 °C for 2 h placed on TZ8Y tape. The pellets were cut to bars (2 mm × 9 mm × 8 mm) and ground to have parallel sides. The samples of ScYSZ were brittle and before cutting they were imbedded in epoxy. The ground pellets were investigated by X-ray diffraction in a STOE STADIP P diffractometer using Cu K $\alpha$ . Before measuring the conductivity, Pt-paste was applied as electrodes and the samples heat-treated at

1000 °C for  $\frac{1}{2}$  h. In the case of ScYSZ, the conductivity was measured first in air then in 9% hydrogen with 3%  $\text{H}_2\text{O}$  and then in air again as a function of time at 1000 °C. For the TZ8Y samples, the conductivity was only measured at 1000 °C in air as a function of time. The conductivity was measured by impedance spectroscopy using a computer controlled Solartron 1260 impedance analyser. The impedance spectra were analysed using EQUIVCRT.<sup>14</sup> The conductivity of undoped ScYSZ has also been measured by the van der Pauw-method<sup>15</sup> on a tape cast sample. van der Pauw measurements were only performed in air.

Samples of ScYSZ and ScYSZ with 2 at.% Al have been investigated in the transmission electron microscope (TEM). The TEMs used are JEOL 3000F and 2000FX both equipped with EDS facilities. The spatial resolution for EDS is a few nm in 3000F and a few tens of nm in 2000FX. Scanning electron microscopy (SEM) has been used to supplement TEM to obtain a more general picture concerning the amount, morphology and distribution of the impurity phase.

## 3. Results and discussion

### 3.1. GDMS and XRD

The zirconia raw materials were analysed for 25 trace elements. The results of the analysis of 13 elements are shown in Table 1. These are the elements where differences appear between TZ8Y and ScYSZ. The main glass forming elements are marked with bold, note that ScYSZ is more impure than TZ8Y and has a much higher content of magnesium, silicon and calcium. The Si content in ScYSZ is 380 ppm compared to 9 ppm for TZ8Y. 380 ppm corresponds to approx. 0.04 wt.% Si, which is a low amount compared to the general trend in literature data, where amounts as 0.3 mol% Si<sup>16</sup> and even as high as 1 wt.% Si are found.<sup>10</sup> Though in many cases the initial amount of Si has not been determined.<sup>8,17,18</sup>

XRD of all the prepared samples showed no signs of impurity peaks or extra peaks at all.

Table 1  
Results of the GDMS analysis

Element	Tosoh TZ8Y	ScYSZ
Li	1.4	0.15
<b>Na</b>	370	370
<b>Mg</b>	2.2	310
<b>Al</b>	11	12
<b>Si</b>	9.0	380
<b>K</b>	1.3	22
<b>Ca</b>	4.1	80
Cr	3.9	10
Mn	0.74	1.5
Fe	23	51
Ni	0.18	8.8
Hf	~1.7 wt.%	~1.5 wt.%
Pb	0.20	0.29

All amounts are in weight ppm, when nothing else is stated.

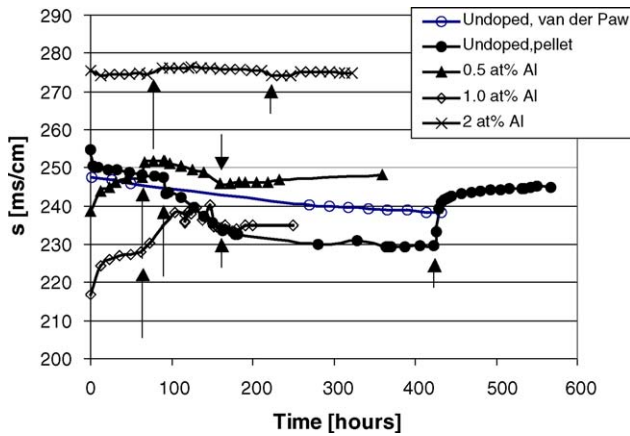


Fig. 1. Conductivity of ScYSZ with different amounts of Al measured at 1000 °C. The long arrows mark the change from oxidising to reducing atmosphere in atmosphere. The short arrows mark the change back to oxidising atmosphere again.

### 3.2. Conductivity

The conductivity of the samples measured at 1000 °C as a function of time is shown in Fig. 1 for ScYSZ and in Fig. 2 for TZ8Y. The arrows in Fig. 1 mark the changes in atmosphere as described above.

As seen in Fig. 1, the conductivity measured by van der Pauw is constantly decreasing over time. The conductivity measured by impedance spectroscopy on a pellet decreases with the same slope as the van der Pauw measurements during the first measurement in air. The bar shaped pellet responds to reducing conditions applied after 90 h showing a decrease in conductivity. However, when exposed to oxidising atmosphere again, the conductivity reaches the same level as before reduction, resulting in no degradation in total. The conductivity in air of the pellet is higher than the conductivity of the tape. Reducing atmosphere seems to have a positive effect on the stabilisation of ScYSZ. It is not expected that stabilised zirconia responds to reduction. Ytria stabilised zirconia is stable down to an oxygen partial pressure below  $10^{-25}$  atm at 1000 °C having a constant conductivity.<sup>19,20</sup> In 9% H<sub>2</sub> in N<sub>2</sub> bubbled through water at 12 °C as used here,

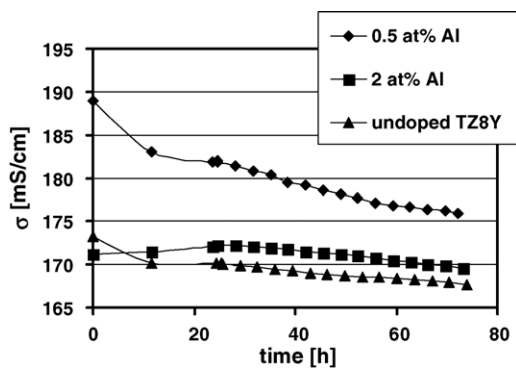


Fig. 2. Conductivity at 1000 °C as a function of time of TZ8Y with and without Al addition.

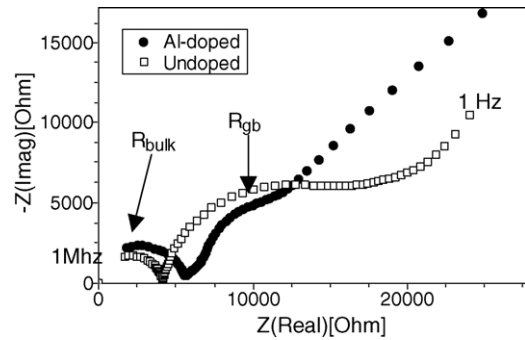


Fig. 3. Impedance spectra of 2 at.% Al-doped ScYSZ (filled symbols) and undoped ScYSZ (open symbols) at 360 °C in air. Both grain boundary and bulk (high frequencies) contribution to the resistivity are seen.

the oxygen partial pressure does not go below  $10^{-20}$  atm. It is earlier seen that transition metal impurities in TZ8Y will rearrange during reduction having a significant influence on the conductivity.<sup>21</sup> Here impurities that could respond to reduction such as iron, nickel and chromium are present.

The conductivity of ScYSZ with 2 at.% Al is significantly higher than the conductivity of the other compositions. In order to investigate why this difference occur, the conductivity has been measured by impedance spectroscopy as a function of temperature on flat, pellet shaped samples of equal dimensions both on 2 at.% Al-doped and undoped ScYSZ. Fig. 3 shows the impedance spectra at 368 °C. Values for the conductivity found by fitting these impedance spectra are given in Table 2. At this temperature both bulk and grain boundary contributions to the resistivity are seen. The bulk resistivity of the 2 at.% Al-doped sample is higher than the bulk resistivity of the undoped sample. This suggests that Al can be dissolved in small amounts in ScYSZ, but causes lattice tensions and trapping of vacancies due to the smaller ionic radius reducing the conductivity. However, the grain boundary resistivity of the undoped sample is much higher than the grain boundary resistivity of the 2 at.% Al-doped sample resulting in a higher total conductivity of the 2 at.% Al-doped sample.

In the case of TZ8Y, the optimum amount of dopant is 0.5 at.% Al see Fig. 2. However, the conductivity still degrades over time as normally seen for TZ8Y. For ScYSZ, the degradation is low and even zero degradation is observed in the case of 2 at.% Al. The conductivity of TZ8Y with and without Al has also been investigated as a function of temperature. The conductivity of 0.5 at.% Al TZ8Y is at all temperatures higher.

Table 2

Bulk and grain boundary conductivity at 368 °C for ScYSZ and 2 at.% Al-doped ScYSZ

Sample	$\sigma_{\text{bulk}}$ (S/cm)	$\sigma_{\text{gb}}$ (S/cm)	$\sigma_{\text{total}}$ (S/cm)
Undoped ScYSZ	2.41E-05	8.79E-06	6.44E-06
2 at.% Al-doped ScYSZ	1.93E-05	1.31E-04	1.69E-04

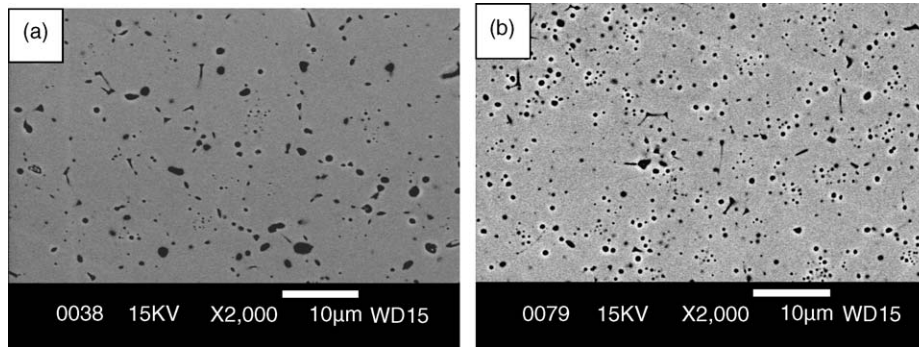


Fig. 4. SEM pictures showing the microstructure of (a) 2 at.% Al-doped ScYSZ and (b) undoped ScYSZ. The theoretical density of the samples is >98% hence the dark spots are inclusions not porosity. The dark spots surrounded by bright lines are generally holes left by inclusions that are pulled out from the material during preparation.

The difference in optimum Al-content between TZ8Y and ScYSZ is consistent with the GDMS results showing that ScYSZ contains more impurities and especially more Si than TZ8Y. It is, therefore, expected that less Al is required for scavenging in TZ8Y. The increase in Al-content does not correspond one to one with the difference in Si-content. There is about 40 times more Si in ScYSZ than in TZ8Y, but only four times more aluminium is needed for scavenging. When comparing to literature data on Tosoh TZ8Y it is found that 1.2 at.%<sup>8</sup> and 1 at.%<sup>17</sup> are optimal for scavenging of Si, which is close to the amount found here considering the different sample processing parameters.

### 3.3. SEM and TEM

Generally two types of impurity-containing ( $\text{SiO}_2$ ,  $\text{Na}_2\text{O}$ ,  $\text{Al}_2\text{O}_3$ ,  $\text{MgO}$ ,  $\text{K}_2\text{O}$ ,  $\text{CaO}$ ) inclusions are present in stabilized zirconia. Some of the impurities are collected in round-shaped crystalline particles present within grains and on grain boundaries. The other type is an amorphous phase present as films (seen as lines in micrographs) along grain boundaries and in triple points. The latter type is a grain boundary (GB) glass phase and is known to influence grain boundary conductivity of stabilized zirconia.<sup>22,23</sup> The presence of two types of inclusions in Al doped stabilised zirconia is reported in literature.<sup>22,24</sup> This pattern is also seen in the present samples, both in ScYSZ and TZ8Y undoped and doped with alumina, as revealed by SEM in Fig. 4(a) and (b) and by TEM in Fig. 5. EDS analysis shows that the chemical composition of both crystalline and amorphous phases varies in a large range even in the same sample (see Table 3).

SEM and TEM also show that doping with Al changes the microstructures of ScYSZ and TZ8Y significantly with respect to the distribution, morphology, relative amount and chemical composition of the two types of inclusions. In the following the results obtained from ScYSZ are used to illustrate these changes.

Fig. 4(a) and (b) show the typical microstructure of 2 at.% Al ScYSZ and undoped ScYSZ. Although the samples have not been etched to accentuate the grain boundaries it is seen

that the grains in 2 at.% Al ScYSZ are larger. The impurity inclusions are larger as well indicating that the impurities are gathered in larger but fewer areas. The length of the GB glass film per unit area measured on SEM micrographs ( $L_A$  in Table 4) decreases by almost 50% in 2 at.% Al ScYSZ. These microstructural changes correlate well with the decrease of grain boundary resistivity in 2 at.% Al ScYSZ mentioned above.

One of the explanations is that the decrease of the length of the GB glass film in 2 at.% Al ScYSZ is related to a change of the morphology of the glass film as shown by TEM micrographs in Fig. 6. The GB glass phase in the case of ScYSZ-2 at.% Al is thicker and shorter. The measured aspect ratio of the GB glass phase (length/maximum thickness) is around 5 for 2 at.% Al ScYSZ and 10 for undoped ScYSZ (see

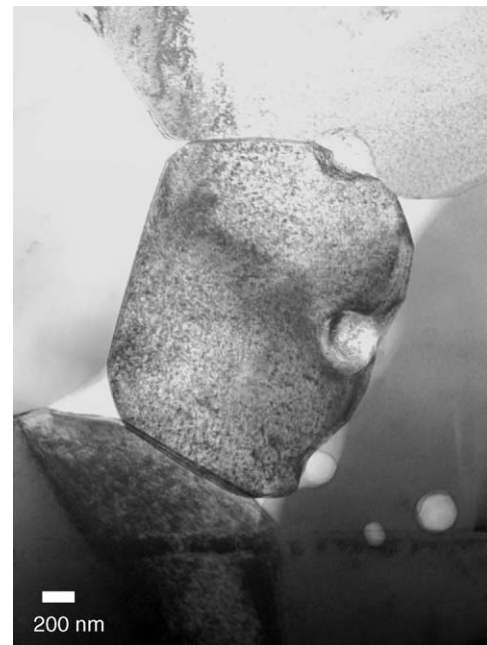


Fig. 5. TEM picture of grain in undoped ScYSZ illustrating the two different types of inclusions, the round crystalline particles and the glassy triple points, found in the materials.



Table 3

The chemical constituents of both grain boundary glass phases and crystalline round inclusions in ScYSZ and 2 at.% Al-doped ScYSZ

Sample	GB glass film (Zr < 10 at.%)	Crystalline round particle	Particle $A_f$ (%)
ScYSZ	Si–Al–Na–Mg Si–Al–Na–Mg–Ca (Si ~ 90, Al 1–2)	Zr–Si–Ca Zr–Si–Al–Na–Mg (Zr-rich, Al < 1, Si < 1)	2.6
ScYSZ + 2 at.% Al	Si–Al (Na) (Si ~ 70, Al 20–30)	Al–Si–Na Al–Si–Mg Al–Si–Na–Mg Al–Si–Na–Mg–K–Ca (Al 10–80 at.%, Si 1–11 at.%)	3.1

The area fraction of crystalline articles,  $A_f$ , is also given.

Table 4

Results of the EDS analysis of the grain boundary glass phase in two of the ScYSZ samples

Sample	Grain boundary glass film (mol%)	$L_A$ of GB glass ( $\mu\text{m}/\mu\text{m}^2$ )	Aspect ratio of GB glass
ScYSZ	SiO <sub>2</sub> 95.9, Na <sub>2</sub> O 0.2, Al <sub>2</sub> O <sub>3</sub> 0.5, MgO 2.1, CaO 1.3 (by TEM) SiO <sub>2</sub> 92.8, Na <sub>2</sub> O 2.8, Al <sub>2</sub> O <sub>3</sub> 2.3, MgO 2.0 (by SEM)	0.011	10.3
ScYSZ + 2 at.% Al	SiO <sub>2</sub> 73.3, Na <sub>2</sub> O 0.9, Al <sub>2</sub> O <sub>3</sub> 25.8 (by TEM) (too small for SEM)	0.006	4.6

The measured length of GB glass phase per unit area  $L_A$ , the aspect ratio between length and thickness of the glass phase, and the estimated grain size of the matrix are also given.

**Table 4**). This indicates a lower wettability of the glass phase to the grain boundaries of ScYSZ at the sintering temperature as result of Al doping. This difference in glass property may well be related to the variations in chemical composition, which are given also in **Table 4**. The GB glass of 2 at.% Al ScYSZ contains much more Al and much less Si than that in undoped ScYSZ. It has been reported that addition of Al<sub>2</sub>O<sub>3</sub> in a SiO<sub>2</sub>–Na<sub>2</sub>O glass increases the surface tension as well as the viscosity<sup>25</sup> of the glass at certain temperatures.

Another reason for the decrease of the GB glass film in the 2 at.% Al ScYSZ is the scavenging effects of alumina.<sup>2</sup> By analyzing a relatively large number of the two types of impurity inclusions in SEM, it is seen that Al doping not only changes the composition of the GB glass as discussed above

but also changes remarkably the composition of the round-shaped crystalline particles (see **Table 3**). In the undoped ScYSZ a majority of the round particles are the Zr-rich type, which has very low capacity of capturing impurities, i.e. the content of impurities such as Si, Al, Na, . . . in these particles is generally less than 1 at.% each. This is in agreement with the observation of Guo and Yuan.<sup>24</sup> In 2 at.% Al ScYSZ Al-rich particles, which have much higher capacity of capturing impurities than Zr-rich ones, replace a substantial number of Zr-rich particles. The Si content in the Al-rich particles can be as high as 11 at.%. Moreover, it is measured that the fraction of the round particles is increased in the 2 at.% Al ScYSZ (see **Table 3**). Thus compared to undoped ScYSZ more Si is fixed in the crystalline particles in 2 at.% Al ScYSZ and

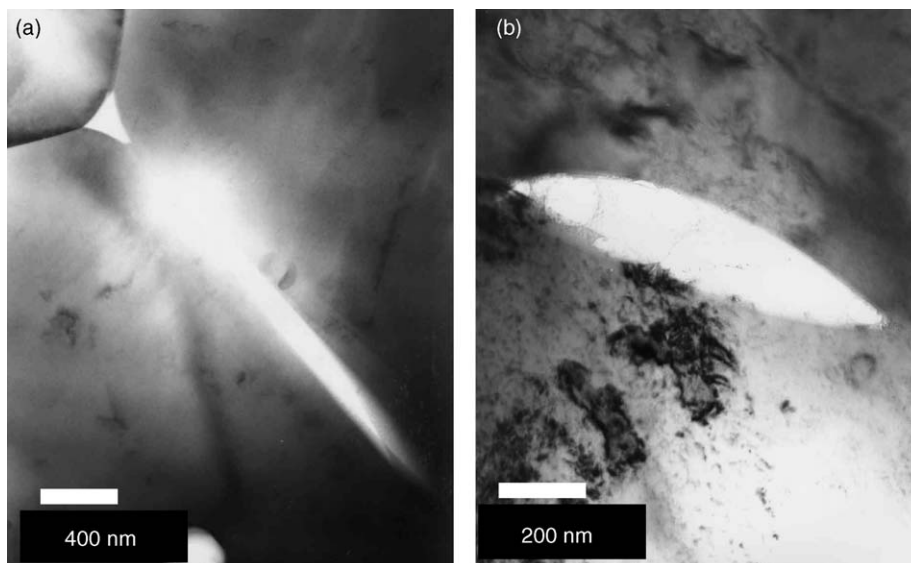


Fig. 6. TEM pictures of grain boundary glass films in (a) ScYSZ and (b) ScYSZ with 2 at.% Al. Note, the scale is not the same for the two pictures.

the amount of Si that is left for forming GB glass phase is reduced. The same trend is seen by Butler and Drennan<sup>2</sup> and by Guo and Tang.<sup>12</sup>

#### 4. Conclusion

The reason for the contradicting results in literature about the effects of alumina doping on the conductivity of stabilized zirconia is better understood and verified by new experimental results obtained on  $\text{Sc}_{0.16}\text{Y}_{0.04}\text{Zr}_{0.80}\text{O}_{2-\delta}$  and Tosoh TZ8Y.

Adding alumina to stabilized zirconia decreases slightly the bulk conductivity, and its influence on the grain boundary conductivity can be positive or negative depending on the amount of alumina addition relative to the amount of impurities (Si, Na, Ca, Mg, K, . . .) present in the material. To increase the overall conductivity an optimum addition of alumina is essential.

SEM, TEM and EDS were used to investigate the beneficial effects of alumina addition to the grain boundary conductivity. Alumina not only “scavenges” impurities into crystalline particles and reduces the amount of grain boundary glass phase, but also changes the chemical composition and reduces the wettability of the grain boundary glass phase.

#### Acknowledgement

The work on ScYSZ was performed under the EU-contract: ENK5-CT-1999-00003.

#### References

- Radford, K. C. and Bratton, R. J., Part 1. Sintering studies. *J. Mater. Sci.*, 1979, **14**, 59–65.
- Butler, E. P. and Drennan, J., Microstructural analysis of sintered high-conductivity zirconia with  $\text{Al}_2\text{O}_3$  additions. *J. Am. Ceram. Soc.*, 1982, **65**(10), 474–478.
- Drennan, J. and Butler, E. P., Does alumina act as a grain boundary scavenger in zirconia? *Science of Ceramics 12*. Faenza, Italy, 1984, pp. 267–272.
- Tsukuma, Ueda, E. and Shimada, M., *J. Am. Ceram. Soc.*, 1985, **68**(1), C4.
- Badwal, S. P. S., Effect of alumina and monoclinic zirconia on the electrical conductivity of  $\text{Sc}_2\text{O}_3\text{-ZrO}_2$  compositions. *J. Mater. Sci.*, 1983, **18**, 3230–3242.
- Bernard, H., *Report CEA-R-5090 Commissariat a l'energie atomique CEN-Saelay*, France, April 1981.
- Verkerk, M. J., Winnubst, A. J. A. and Burggraaf, A. J., Effect of impurities on sintering and conductivity of yttria-stabilised zirconia. *J. Mater. Sci.*, 1982, **17**, 3113–3122.
- Feighery, A. J. and Irvine, J. T. S., Effect of alumina additions on electrical properties of 8 mol% yttria-stabilised zirconia. *Solid State Ionics*, 1999, **121**, 209–216.
- Butler, E. P. and Bonanos, N., The characterization of  $\text{ZrO}_2$  engineering ceramics by A.C. impedance spectroscopy. *Mater. Sci. Ing.*, 1985, **71**, 49–56.
- Rizea, A., Chirlesan, D., Petot, C. and Petot-Ervias, G., The influence of alumina on the microstructure and grain boundary conductivity of yttria-doped zirconia. *SSI*, 2002, **146**, 341–353.
- Miyayama, M., Yanagida, H. and Asada, A., Effects of  $\text{Al}_2\text{O}_3$  addition on reactivity and microstructure of yttria-stabilised zirconia. *Am. Ceram. Soc. Bull.*, 1985, **64**(4), 660–664.
- Guo, X., Tang, C.-Q. and Yuan, R.-Z., Grain boundary ionic conductivity in zirconia-based solid electrolyte with alumina addition. *J. Eur. Ceram. Soc.*, 1995, **15**, 25–32.
- Shannon, R. D., Revised effective ionic radii and systematic studies of interatomic distances in halides and chalcogenides. *Acta Cryst.*, 1976, **A32**, 751.
- Boukamp, B. A., *EQUIVALENT CIRCUIT (EQUICRT.PAS)*, Users Manual (2nd revised version). Report CT88/265/128, University of Twente, 53 pp.
- van der Pauw, L. J., *Philips Res. Rep.*, 1958, **13**, 1.
- Butler, E. P. and Drennan, J., Microstructural analysis of sintered high conductivity zirconia with  $\text{Al}_2\text{O}_3$  additions. *J. Am. Ceram. Soc.*, 1982, **65**(10), 474–478.
- Hassan, A. A. E., Menzler, N. H., Blass, G., Ali, M. E., Buchkremer, H. P. and Stöver, D., Influence of alumina dopant on the properties of yttria-stabilised zirconia for SOFC applications. *J. Mater. Sci.*, 2002, **37**, 3467–3475.
- Ji, Y., Liu, J., Lü, Z., Zhai, X., He, T. and Su, W., Study on the properties of  $\text{Al}_2\text{O}_3$ -doped  $(\text{ZrO}_2)_{0.92}(\text{Y}_2\text{O}_3)_{0.08}$  electrolyte. *SSI*, 1999, **126**, 227–283.
- Park, J.-H. and Blumenthal, R. N., Electronic transport in 8 mole percent  $\text{Y}_2\text{O}_3\text{-ZrO}_2$ . *J. Electrochem. Soc.*, 1989, **136**(10), 2867–2876.
- Etsell, T. H. and Flengas, S. N., The electrical properties of solid oxide electrolytes. *Chem. Rev.*, 1970, **70**(3), 339–376.
- Linderth, S., Bonanos, N., Jensen, K. V. and Bilde-Sørensen, J., Effect of NiO-to-Ni transformation on conductivity and structure of yttria-stabilized  $\text{ZrO}_2$ . *J. Am. Ceram. Soc.*, 2001, **84**(11), 2652–2656.
- Apel, C. C. and Bonanos, N., Structural and electrical characterisation of silica-containing yttria-stabilised zirconia. *J. Eur. Ceram. Soc.*, 1999, **19**, 847–851.
- Martin, M. C. and Mecartney, M. L., Grain boundary ionic conductivity of yttrium stabilised zirconia as a function of silica content and grain size. *SSI*, 2003, **161**, 67–79.
- Guo, X. and Yuan, R., Roles of alumina in zirconia-based solid electrolyte. *J. Mater. Sci.*, 1995, **30**, 923–931.
- Holland, L., *The Properties of Glass Surfaces*. Chapman and Hall, London, 1964.